

Supplementary Materials: Enhanced In Vitro Antitumor Activity of GnRH-III-Daunorubicin Bioconjugates Influenced by Sequence Modification

Sabine Schuster, Beáta Biri-Kovács, Bálint Szeder, László Buday, János Gardi, Zsuzsanna Szabó, Gábor Halmos and Gábor Mező

Table of Content

Synthesis strategy of bioconjugate 13	3
RP-HPLC profile and ESI-ion trap mass spectrum of GnRH-III-[⁸ Lys(Dau=Aoa)] (K1).....	4
RP-HPLC profile and ESI-ion trap mass spectrum of GnRH-III-[⁴ Lys(Bu), ⁸ Lys(Dau=Aoa)] (K2).....	4
RP-HPLC profile and ESI-ion trap mass spectrum of GnRH-III-[³ Trp, ⁸ Lys(Dau=Aoa)] (1).....	4
RP-HPLC profile and ESI-ion trap mass spectrum of GnRH-III-[³ D-Tic, ⁸ Lys(Dau=Aoa)] (2).....	5
RP-HPLC profile and ESI-ion trap mass spectrum of GnRH-III-[² ΔHis, ³ D-Tic, ⁸ Lys(Dau=Aoa)] (3).....	5
RP-HPLC profile and ESI-ion trap mass spectrum of GnRH-III-[³ D-Tic, ⁷ D-Trp ⁸ Lys(Dau=Aoa)] (4).....	5
RP-HPLC profile and ESI-ion trap mass spectrum of GnRH-III-[² ΔHis, ³ D-Tic, ⁷ D-Trp ⁸ Lys(Dau=Aoa)] (5).....	6
RP-HPLC profile and ESI-ion trap mass spectrum of GnRH-III-[⁶ Asp(OMe), ⁸ Lys(Dau=Aoa)] (6).....	6
RP-HPLC profile and ESI-ion trap mass spectrum of GnRH-III-[⁸ Lys(Dau=Aoa), ¹⁰ ΔGly-NH-Et] (7).....	6
RP-HPLC profile and ESI-ion trap mass spectrum of GnRH-III-[³ Trp, ⁴ Lys(Bu), ⁸ Lys(Dau=Aoa)] (8).....	7
RP-HPLC profile and ESI-ion trap mass spectrum of GnRH-III-[³ D-Tic, ⁴ Lys(Bu), ⁸ Lys(Dau=Aoa)] (9).....	7
RP-HPLC profile and ESI-ion trap mass spectrum of GnRH-III-[² ΔHis, ³ D-Tic, ⁴ Lys(Bu), ⁸ Lys(Dau=Aoa)] (10).....	7
RP-HPLC profile and ESI-ion trap mass spectrum of GnRH-III-[³ D-Tic, ⁴ Lys(Bu), ⁷ D-Trp ⁸ Lys(Dau=Aoa)] (11).....	8
RP-HPLC profile and ESI-ion trap mass spectrum of GnRH-III-[² ΔHis, ³ D-Tic, ⁴ Lys(Bu), ⁷ D-Trp ⁸ Lys(Dau=Aoa)] (12).....	8
RP-HPLC profile and ESI-ion trap mass spectrum of GnRH-III-[⁴ Lys(Bu), ⁶ Asp(OMe), ⁸ Lys(Dau=Aoa)] (13).....	8
RP-HPLC profile and ESI-ion trap mass spectrum of GnRH-III-[⁴ Lys(Bu), ⁸ Lys(Dau=Aoa), ¹⁰ ΔGly-NH-Et] (14).....	9
Stability of the bioconjugates K2 and 10 in human plasm.....	9
Fragments of K2 and 10 produced in the presence of rat liver homogenate.....	10
Cellular uptake of K2 and 10 by flow cytometry.....	10

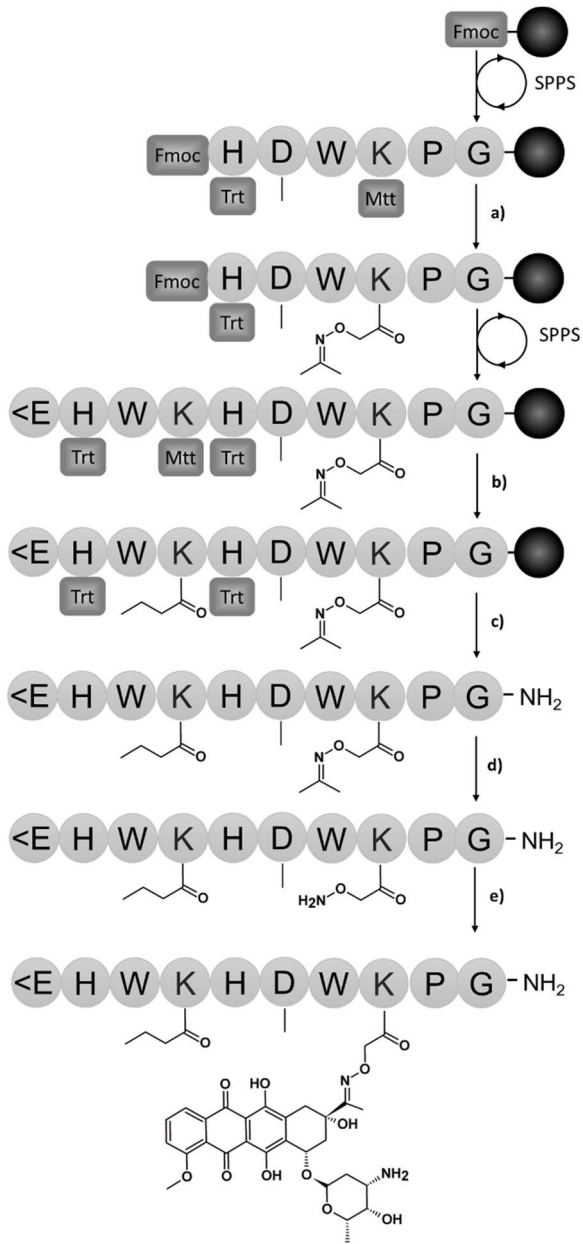


Figure S1. Synthesis strategy for **13** ($<\text{EHWK(Bu)HD(OMe)WK(Dau=Aoa)PG-NH}_2$). Bioconjugate **13** was prepared by manual SPPS according to Fmoc/tBu chemistry on a Rink-Amide MBHA resin (0.73 mmol/g coupling capacity). The general protocol for the synthesis started with DMF-washing (4 x 1 min), followed by Fmoc deprotection with 2% piperidine, 2% DBU in DMF (4 times; 2 + 2 + 5 + 10 min). The coupling reaction was performed by using 3 eq of α -Fmoc-protected amino acid derivative, 3 eq DIC and 3 eq HOEt in DMF (60 min). After washing with DMF (3 x 1 min) and DCM (2 x 1 min) the success of the coupling was controlled by ninhydrin test.

a)(1) 2% TFA in DCM - 6x5 min; (2) 10% DIPEA in DCM - 3x5 min; (3) 10 eq $\geq\text{Aoa-OH}$, 10 equiv K-Oxima pure \circledR , 10 eq DIC in DMF – 2 h

b)(1) 2% TFA in DCM - 6x5 min; (2) 10% DIPEA in DCM - 3x5 min; (3) 3 eq butyric anhydride, 3 eq DIPEA in DMF – 2 h

c) 95% TFA, 2.5% TIS, 2.5% H_2O – 2 h

d) 2 M methoxylamine hydrochloride in 0.2 M NH_4OAc -buffer (pH 5) – 2-3 h (reaction control by analytical HPLC)

e) 1.3 equiv Dau in 0.2 M NH_4OAc -buffer (pH 5) – overnight

Aoa: aminoxyacetyl; **Bu:** butyl; **Dau:** daunorubicine; **Fmoc:** 9-fluorenylmethoxycarbonyl; **Mtt:** 4-methyltrityl; **SPPS:** solid phase peptide synthesis; **tBu:** *tert*-butyl; **Trt:** trityl; $\geq:$ isopropylidene; $\bullet:$ Rink-Amide-MBHA-resin; $\bullet:$ amino acid; $\blacksquare:$ protecting group

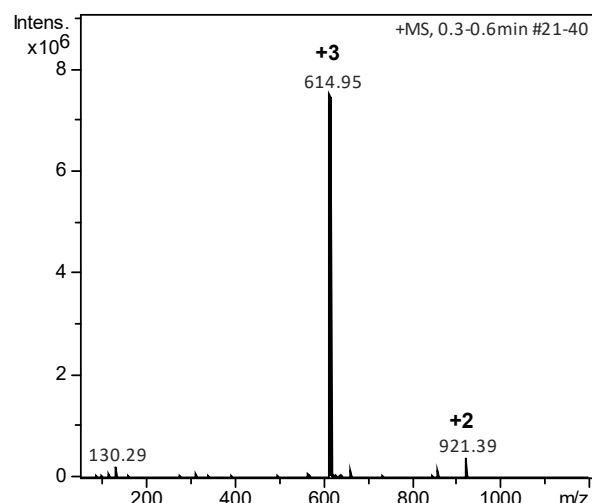
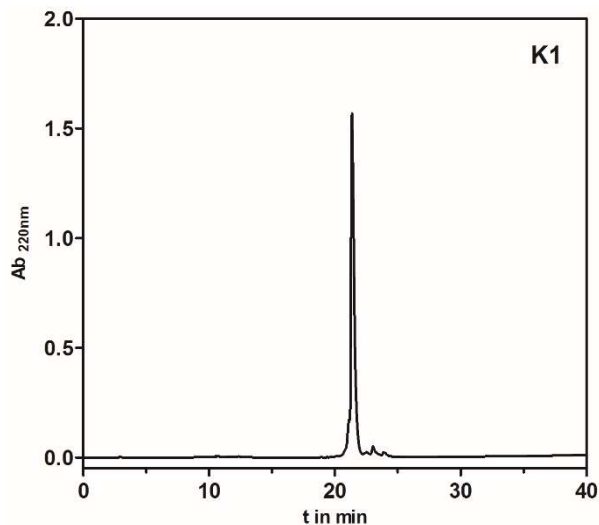


Figure S2. RP-HPLC profile and ESI-ion trap mass spectrum of GnRH-III-[⁴Ser, ⁸Lys(Dau=Aoa)] (**K1**). ($MW_{\text{cal}}/MW_{\text{exp}} = 1841.89/1841.85$ g/mol, *fragment ion: amino sugar loss of Dau)

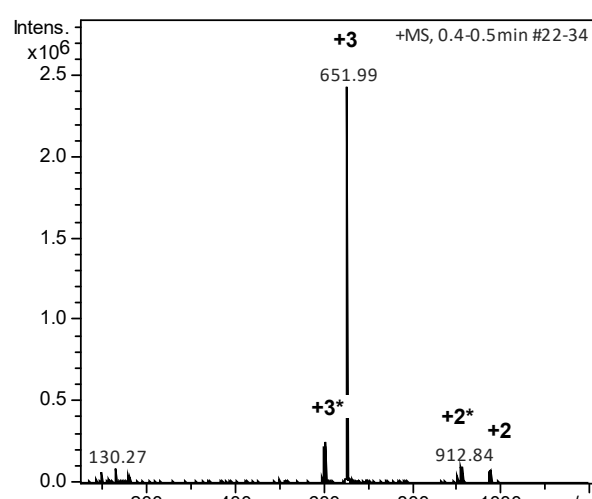
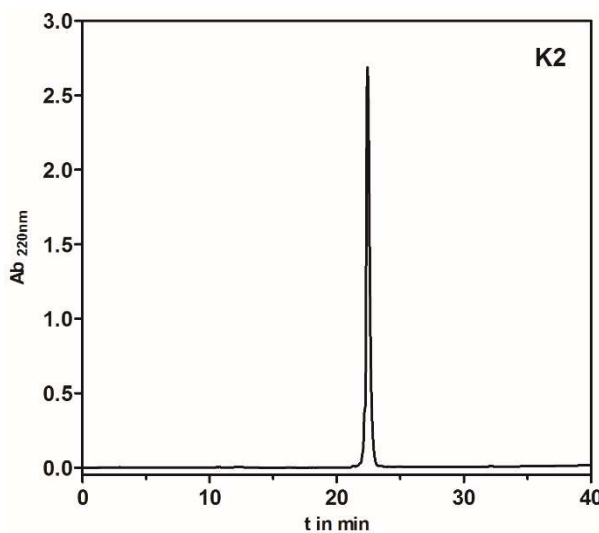


Figure S3. RP-HPLC profile and ESI-ion trap mass spectrum of GnRH-III-[⁴Lys(Bu), ⁸Lys(Dau=Aoa)] (**K2**). ($MW_{\text{cal}}/MW_{\text{exp}} = 1953.07/1952.97$ g/mol).

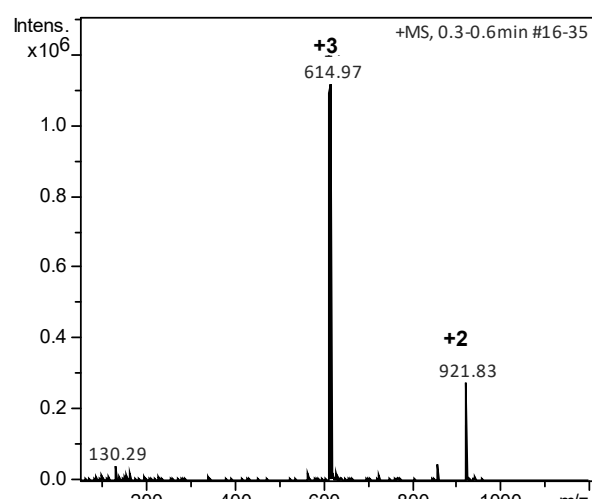
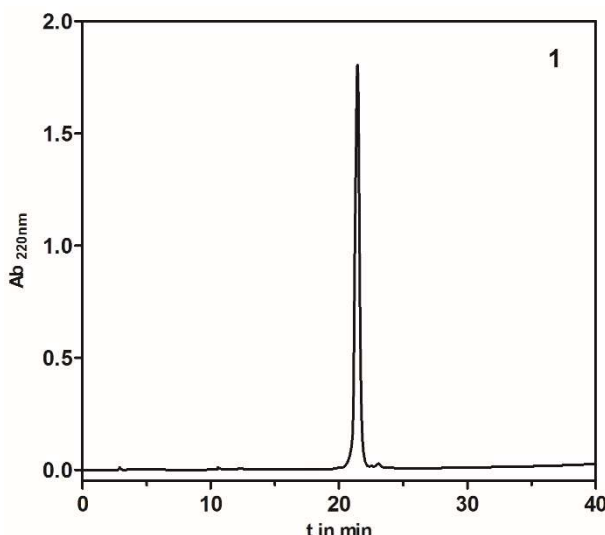


Figure S4. RP-HPLC profile and ESI-ion trap mass spectrum of GnRH-III-[³Trp, ⁸Lys(Dau=Aoa)] (**1**). ($MW_{\text{cal}}/MW_{\text{exp}} = 1841.89/1841.91$ g/mol).

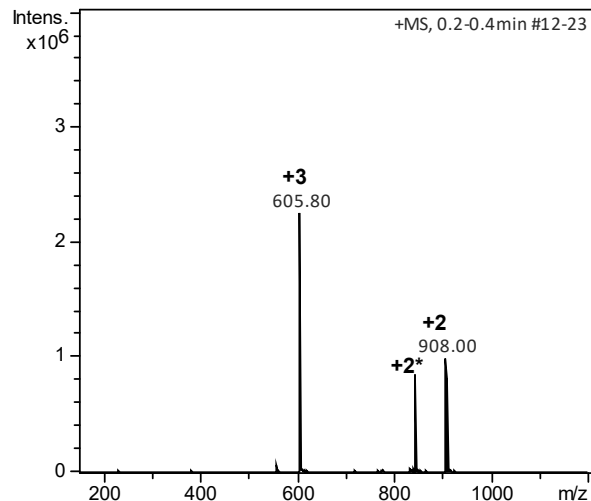
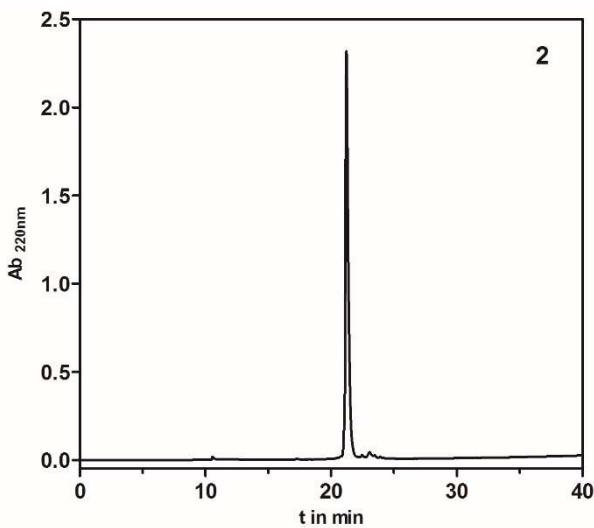


Figure S5. RP-HPLC profile and ESI-ion trap mass spectrum of GnRH-III-[^{3}Tic , $^{8}\text{Lys(Dau=Aoa)}$] (**2**). ($\text{MW}_{\text{cal}} / \text{MW}_{\text{exp}} = 1814.86 / 1814.40 \text{ g/mol}$).

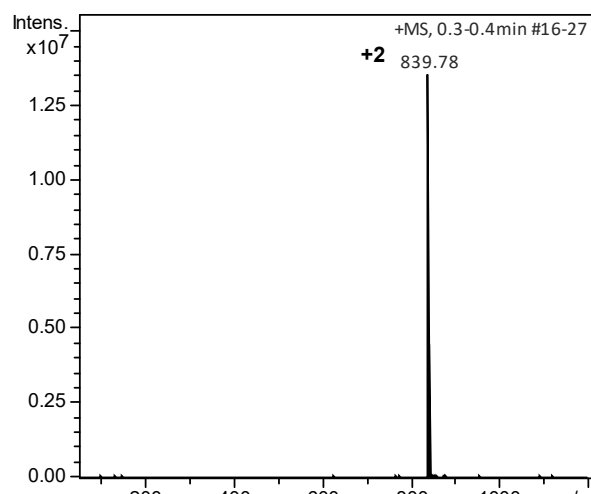
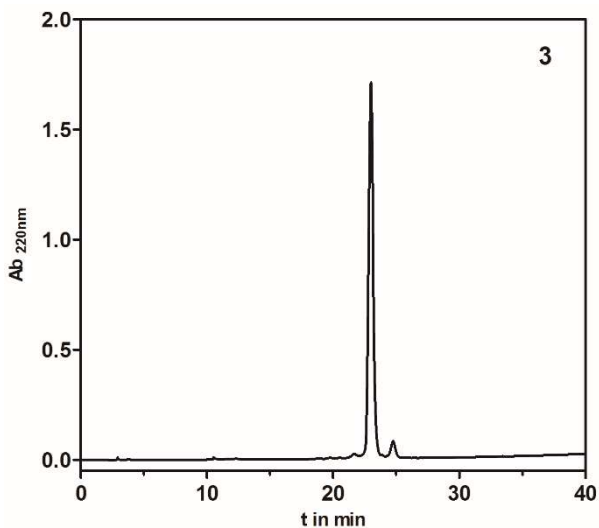


Figure S6. RP-HPLC profile and ESI-ion trap mass spectrum of GnRH-III-[$^{2}\Delta\text{His}$, $^{3}\text{D-Tic}$, $^{8}\text{Lys(Dau=Aoa)}$] (**3**). ($\text{MW}_{\text{cal}} / \text{MW}_{\text{exp}} = 1677.72 / 1677.56 \text{ g/mol}$).

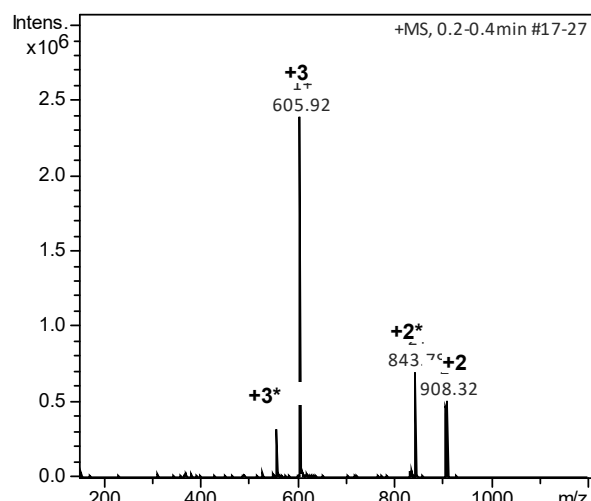
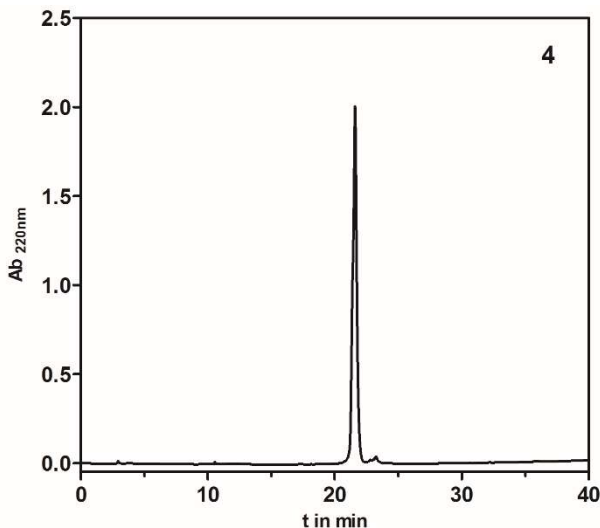


Figure S7. RP-HPLC profile and ESI-ion trap mass spectrum of GnRH-III-[$^{3}\text{D-Tic}$, $^{7}\text{D-Trp}$, $^{8}\text{Lys(Dau=Aoa)}$] (**4**). ($\text{MW}_{\text{cal}} / \text{MW}_{\text{exp}} = 1814.86 / 1814.64 \text{ g/mol}$).

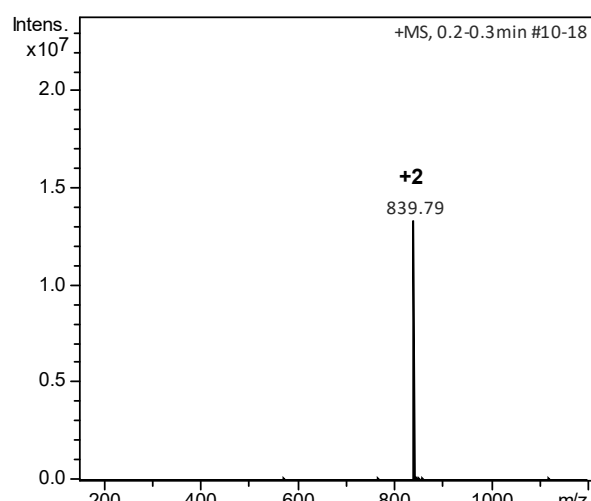
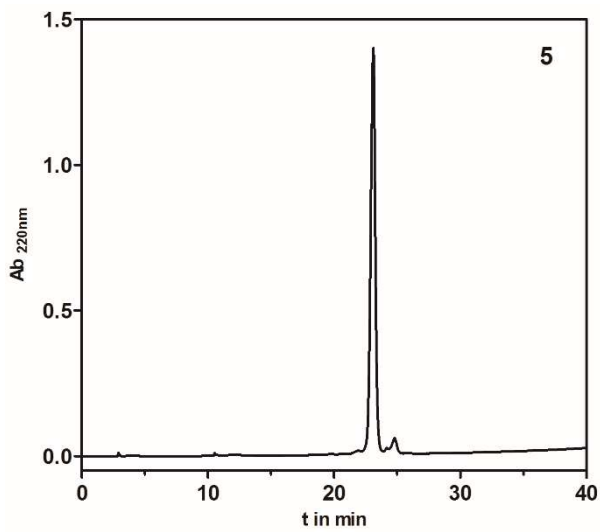


Figure S8. RP-HPLC profile and ESI-ion trap mass spectrum of GnRH-III-[²ΔHis, ³D-Tic, ⁷D-Trp, ⁸Lys(Dau=Aoa)] (**5**). (MW_{cal} /MW_{exp} = 1677.72/1677.58 g/mol).

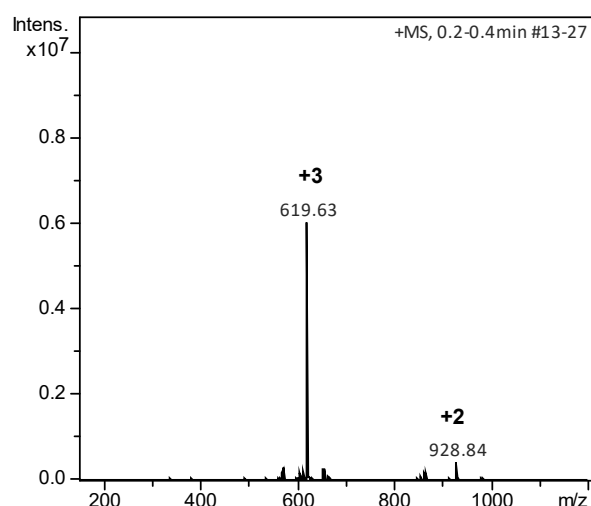
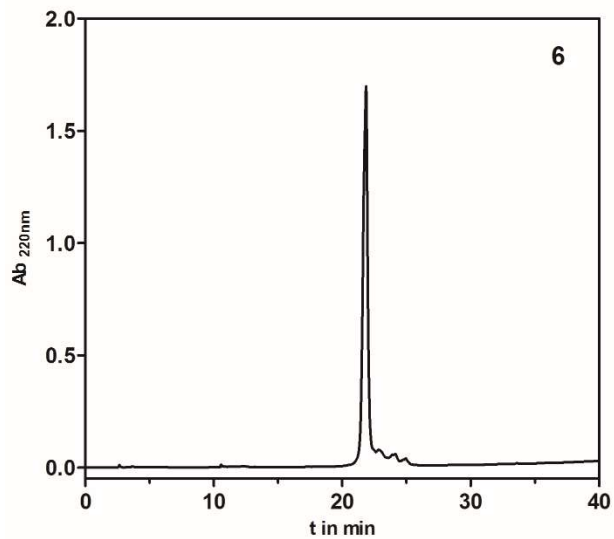


Figure S9. RP-HPLC profile and ESI-ion trap mass spectrum of GnRH-III-[⁶Asp(OMe), ⁸Lys(Dau=Aoa)] (**6**). (MW_{cal} /MW_{exp} = 1855.91/1855.68 g/mol).

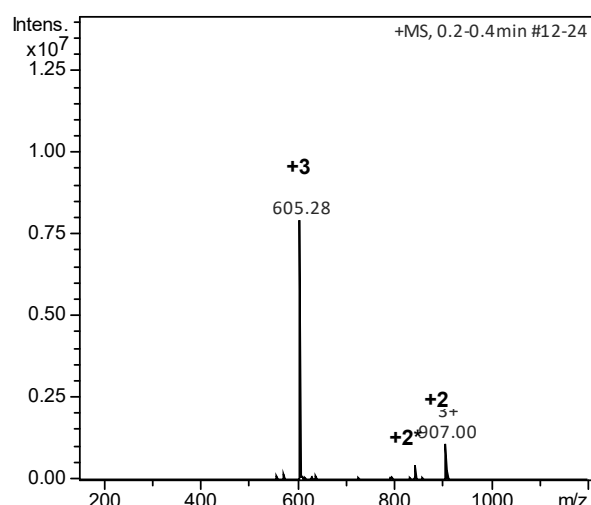
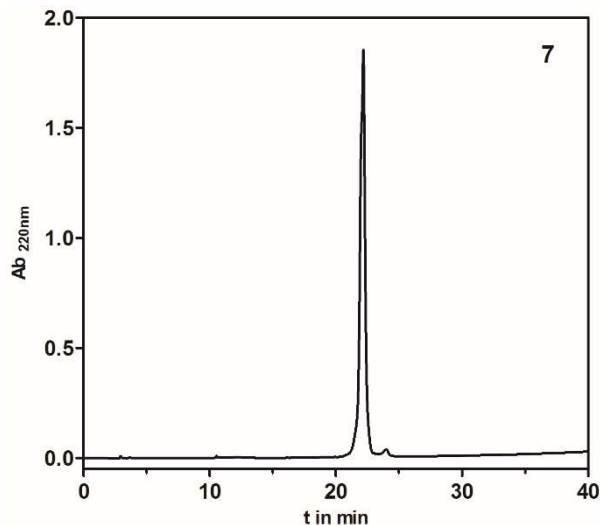


Figure S10. RP-HPLC profile and ESI-ion trap mass spectrum of GnRH-III-[⁸Lys(Dau=Aoa), ¹⁰ΔGly-NH-Et] (**7**). (MW_{cal} /MW_{exp} = 1812.88/1812.84 g/mol).

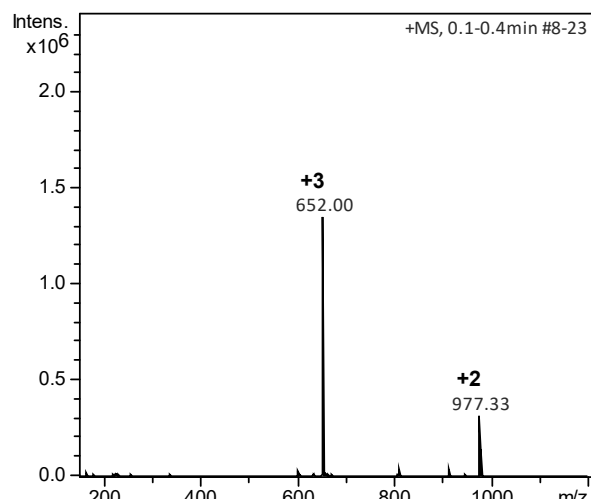
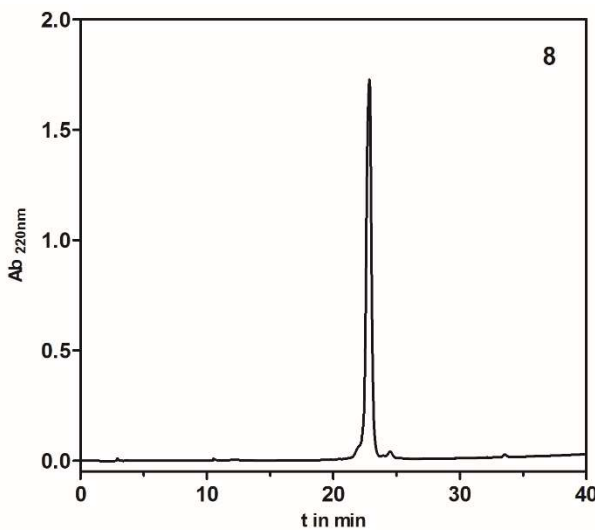


Figure S11. RP-HPLC profile and ESI-ion trap mass spectrum of GnRH-III-[^3D -Trp, $^4\text{Lys(Bu)}$, $^8\text{Lys(Dau=Aoa)}$] (**8**). ($\text{MW}_{\text{cal}}/\text{MW}_{\text{exp}} = 1953.07/1953.00 \text{ g/mol}$).

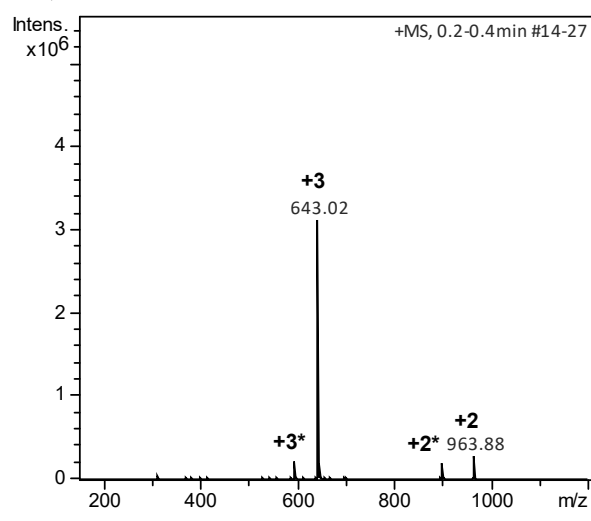
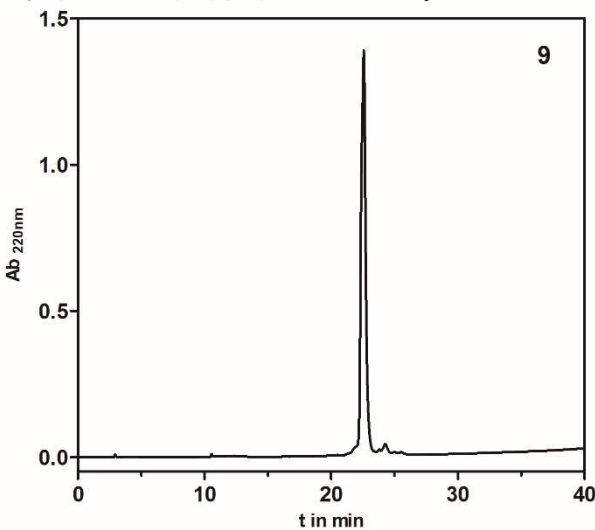


Figure S12. RP-HPLC profile and ESI-ion trap mass spectrum of GnRH-III-[^3D -Tic, $^4\text{Lys(Bu)}$, $^8\text{Lys(Dau=Aoa)}$] (**9**). ($\text{MW}_{\text{cal}}/\text{MW}_{\text{exp}} = 1926.05/1926.06 \text{ g/mol}$).

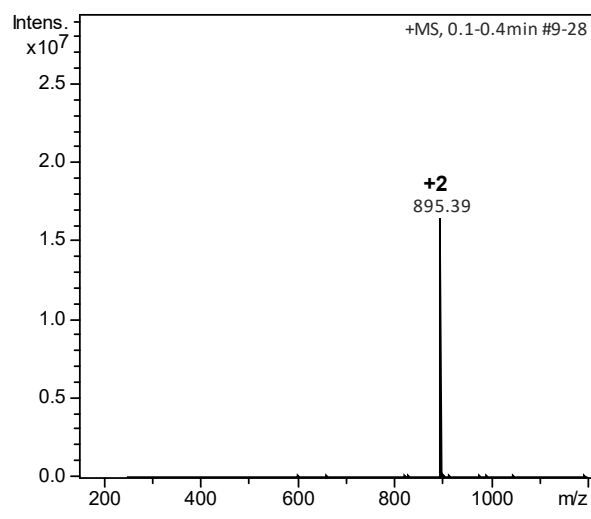
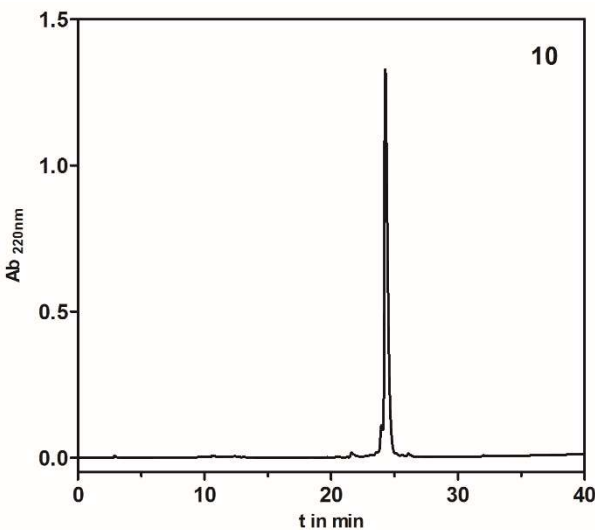


Figure S13. RP-HPLC profile and ESI-ion trap mass spectrum of GnRH-III-[$^2\Delta$ His, ^3D -Tic, $^4\text{Lys(Bu)}$, $^8\text{Lys(Dau=Aoa)}$] (**10**). ($\text{MW}_{\text{cal}}/\text{MW}_{\text{exp}} = 1788.91/1788.78 \text{ g/mol}$).

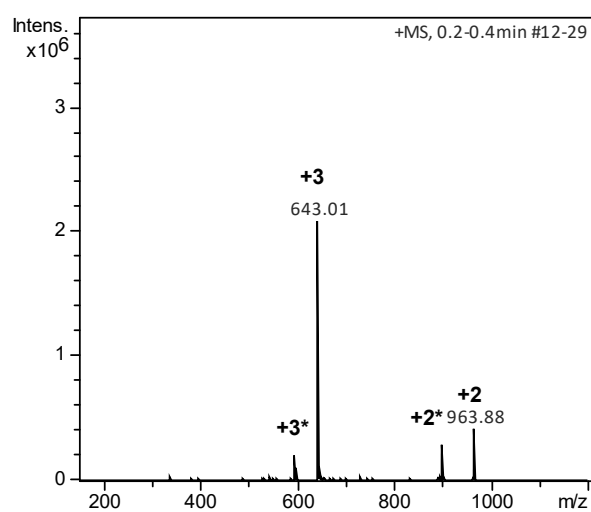
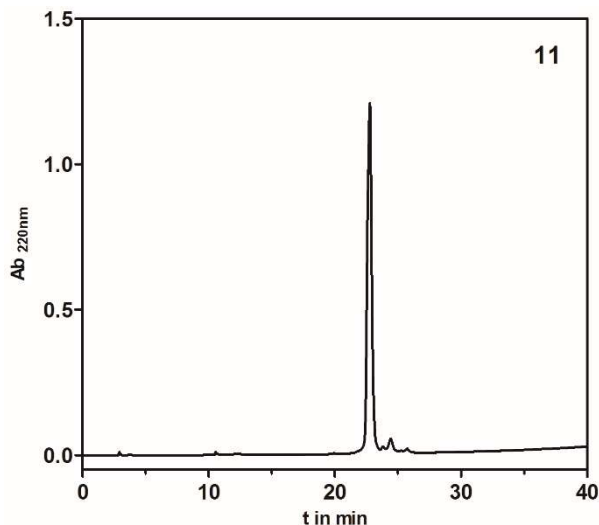


Figure S14. RP-HPLC profile and ESI-ion trap mass spectrum of GnRH-III-[³D-Tic, ⁴Lys(Bu), ⁷D-Trp, ⁸Lys(Dau=Aoa)] (**11**). (MW_{cal} /MW_{exp} = 1926.05/1926.03 g/mol).

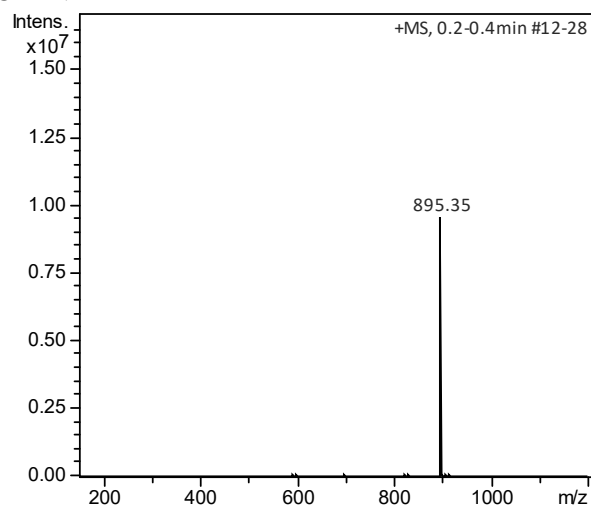
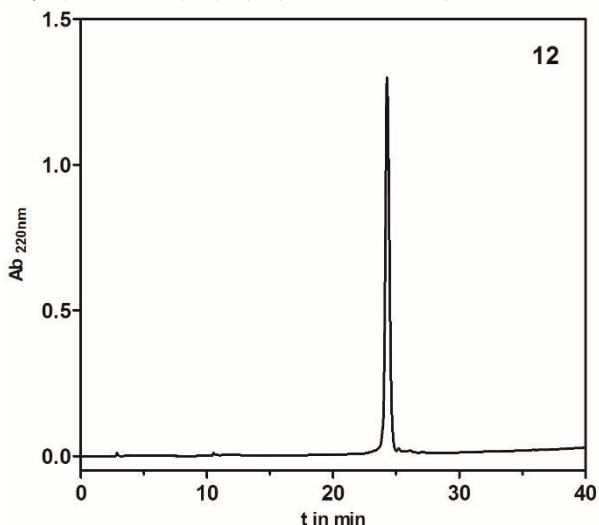


Figure S15. RP-HPLC profile and ESI-ion trap mass spectrum of GnRH-III-[²ΔHis, ³D-Tic, ⁴Lys(Bu), ⁷D-Trp, ⁸Lys(Dau=Aoa)] (**12**). (MW_{cal} /MW_{exp} = 1788.91/1788.70 g/mol).

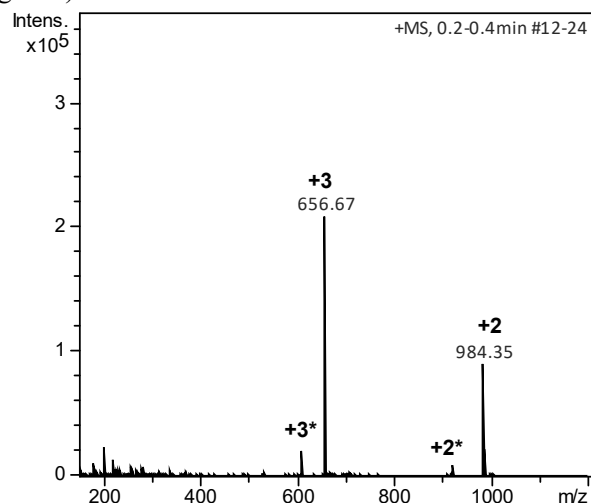
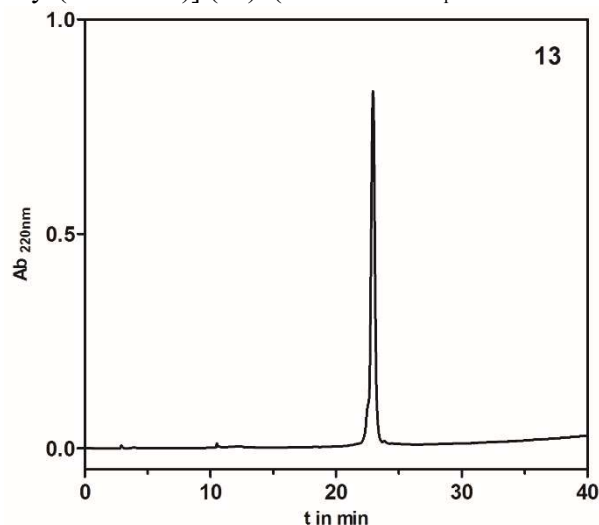


Figure S16. RP-HPLC profile and ESI-ion trap mass spectrum of GnRH-III-[⁴Lys(Bu), ⁶Asp(OMe), ⁸Lys(Dau=Aoa)] (**13**). (MW_{cal} /MW_{exp} = 1967.10/1967.01 g/mol).

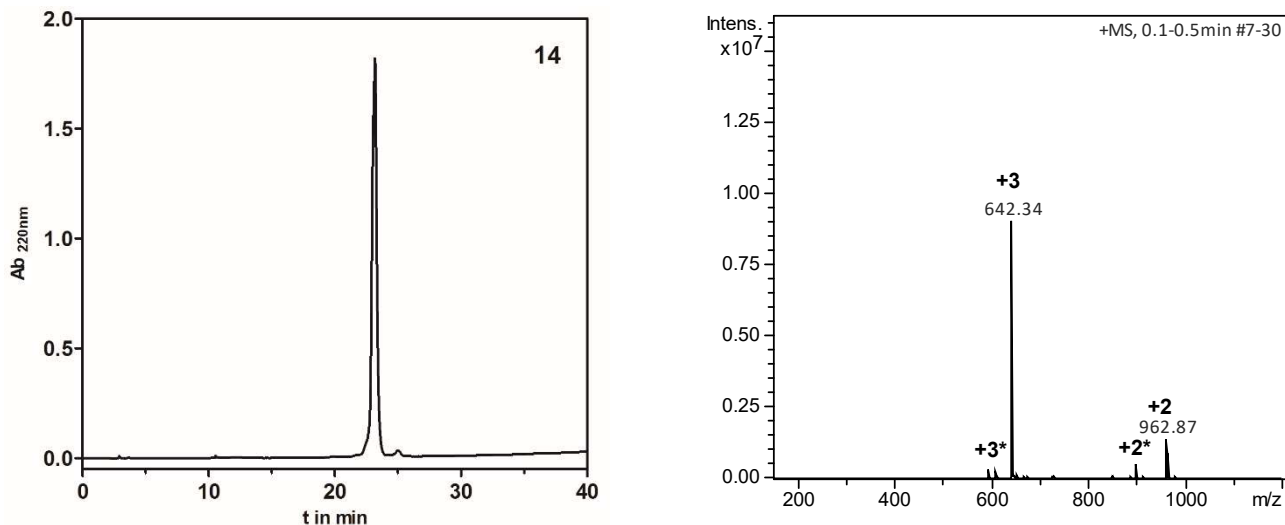


Figure S17. RP-HPLC profile and ESI-ion trap mass spectrum of GnRH-III-[⁸Lys(Dau=Aoa), ¹⁰ΔGly-NH-Et] (**14**). ($MW_{cal}/MW_{exp} = 1924.07/1924.02$ g/mol).

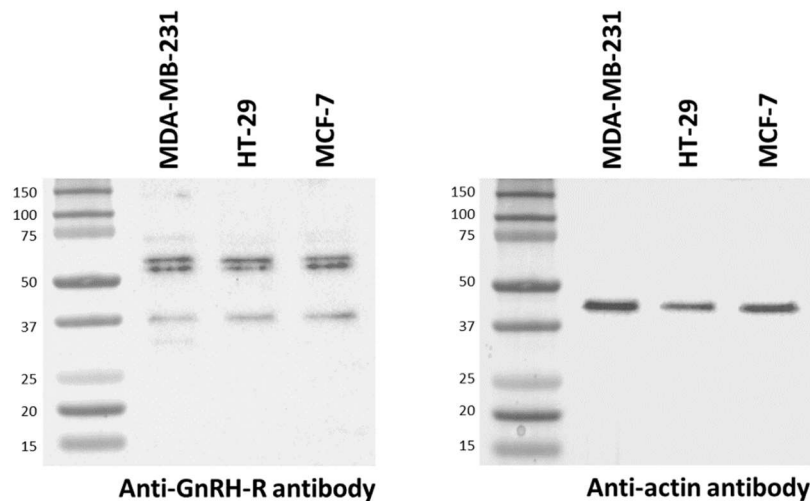


Figure S18. Western blot performed on whole cell lysates of MCF-7 and HT-29 cancer cells. Anti-GnRH-R antibody (Proteintech, 19950-1AP) (left). Actin expression was evaluated as loading control (Santa Cruz Biotechnology, sc-1616 (right)). Band at 38 kDa represents the full length human GnRH-R; the signals at higher molecular weight (55-70 kDa) are assumed to be glycosylated forms of the GnRH-R.

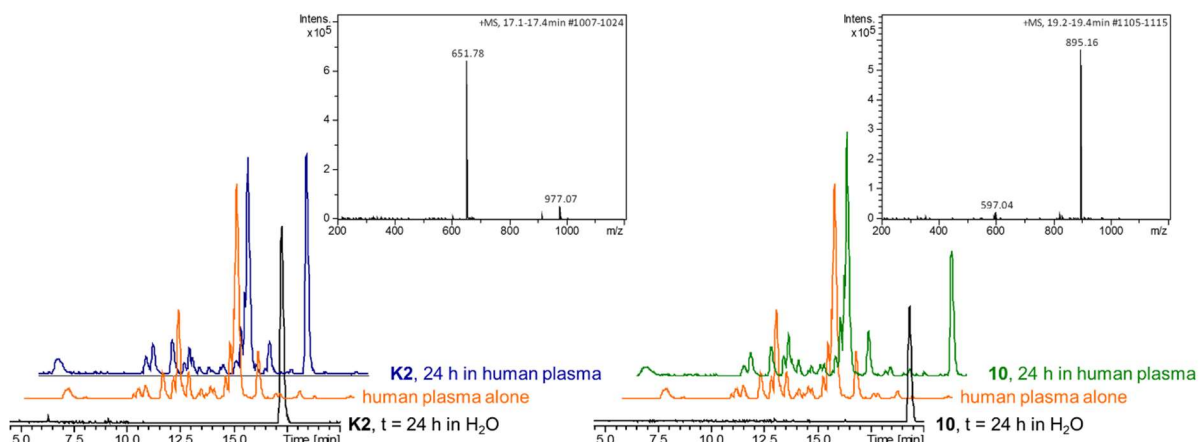


Figure S19. Stability of the bioconjugates **K2** and **10** in human plasma. LC-MS chromatogram of human plasma and the conjugates after 24 h incubation at 37 °C in H₂O or in human plasma plus the corresponding MS compound spectra.

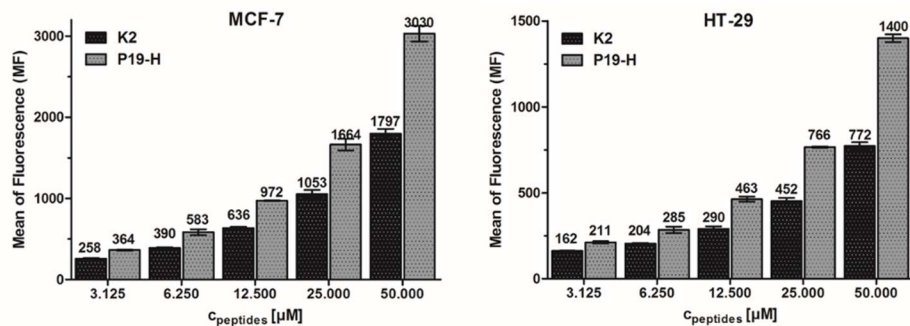


Figure S20. Mean of fluorescence of the cellular uptake of the GnRH-III conjugates **K2** and **10** on MCF-7 and HT-29 cancer cells after 6 h treatment determined by flow cytometry. The cellular uptake of **10** was significantly higher than the uptake of conjugate **K2** for both cells (paired Wilcoxon test, $P=0.002516$ and $P=0.005099$, respectively).

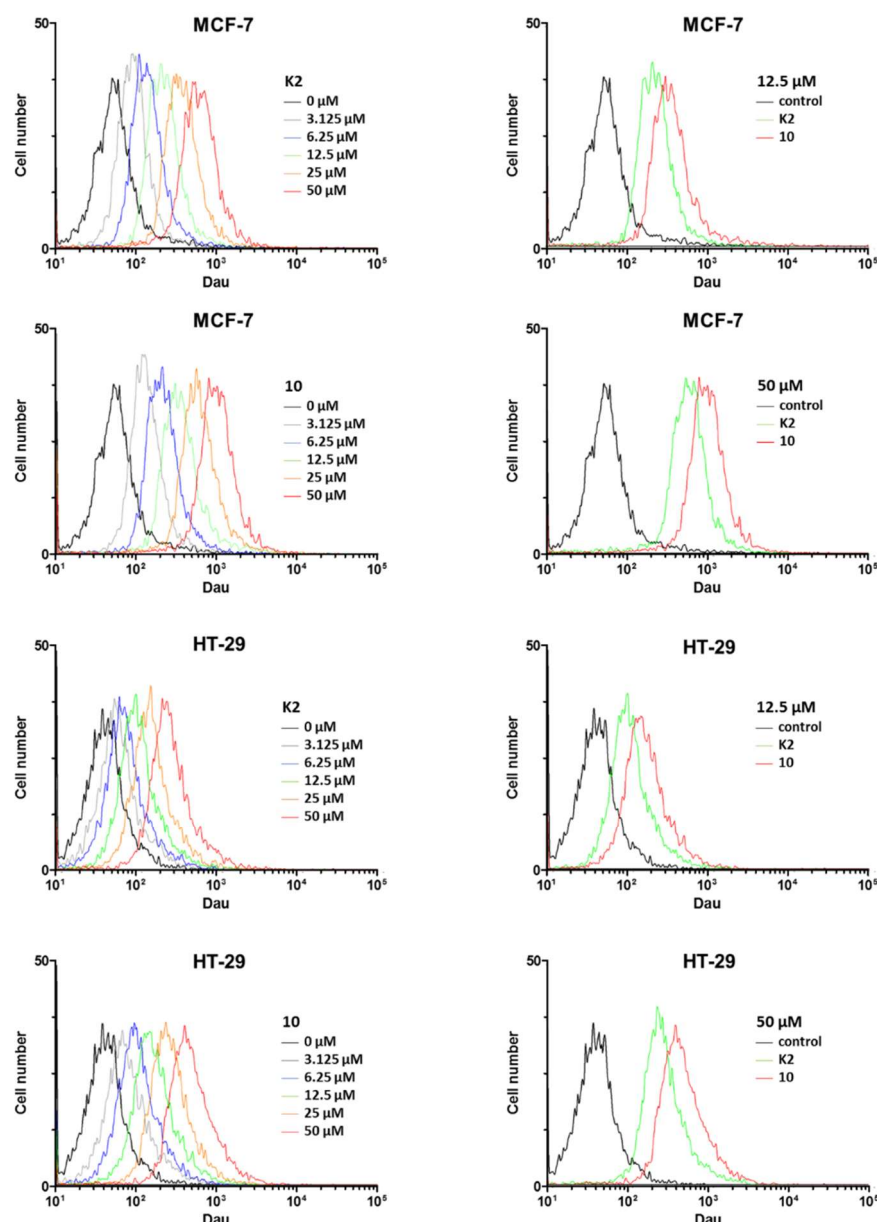


Figure S21. Cellular uptake of the GnRH-III conjugates **K2** and **10** on MCF-7 and HT-29 cancer cells after 6 h treatment determined by flow cytometry. FACS histograms show the concentration dependent cellular uptake.

Table S1. Fragments of GnRH-III-Dau conjugates **K2** and **10** produced by rat liver homogenate

Code	Compound	Fragment	MW_{cal}/MW_{exp}
K2	[⁴ Lys(Bu), ⁸ Lys(Dau=Aoa)]	<EHWK(Bu)HDWK(Dau=Aoa)PG-NH ₂	1953.07/1952.79
		<EHWK(Bu)HDWK(Dau=Aoa)-OH	1799.92/1799.69
		H-HDWK(Dau=Aoa)PG-NH ₂	1320.36/1319.95
		H-HDWK(Dau=Aoa)-OH	1167.18/1166.91
		H-K(Dau=Aoa)PG-NH ₂	881.94/881.44
		H-K(Dau=Aoa)P-OH	825.86/825.40
		H-K(Dau=Aoa)-OH	728.75/728.37
		<EHWK(Bu)HD-OH	902.96/902.84
		<EHWK(Bu)-OH	650.73/650.71
		<EHW-OH	452.46/452.31
10	[² ΔHis, ³ D-Tic, ⁴ Lys(Bu), ⁸ Lys(Dau=Aoa)]	H-DW-OH	319.32/319.27
		<E-D-Tic-K(Bu)HDWK(Dau=Aoa)PG-NH ₂	1788.91/1788.33
		<E-D-Tic-K(Bu)HDWK(Dau=Aoa)-OH	1635.72/1635.22
		<E-D-Tic-K(Bu)HD-OH	738.78/738.26
		<E-D-Tic-K(Bu)H-OH	623.70/623.29
		<E-D-Tic-K(Bu)-OH	486.56/486.90
		H-K(Dau=Aoa)P-OH	825.86/825.40
		H-K(Dau=Aoa)-OH	728.75/728.37